GEOPHYSICS

Intraoceanic subduction spanned the Pacific in the Late Cretaceous–Paleocene

Mathew Domeier,[1]* Grace E. Shephard,[1] Johannes Jakob,[1] Carmen Gaina,[1] Pavel V. Doubrovine,[1] Trond H. Torsvik[1,2,3,4]

The notorious ~60° bend separating the Hawaiian and Emperor chains marked a prominent change in the motion of the Pacific plate at ~47 Ma (million years ago), but the origin of that change remains an outstanding controversy that bears on the nature of major plate reorganizations. Lesser known but equally significant is a conundrum posed by the pre-bend (~80 to 47 Ma) motion of the Pacific plate, which, according to conventional plate models, was directed toward a fast-spreading ridge, in contradiction to tectonic forcing expectations. Using constraints provided by seismic tomography, paleomagnetism, and continental margin geology, we demonstrate that two intraoceanic subduction zones spanned the width of the North Pacific Ocean in Late Cretaceous through Paleocene time, and we present a simple plate tectonic model that explains how those intraoceanic subduction zones shaped the ~80 to 47 Ma kinematic history of the Pacific realm and drove a major plate reorganization.

INTRODUCTION

Following the foundational idea that the Hawaiian-Emperor chain (Fig. 1) is an age-progressive string of volcanic features marking the drift of the Pacific plate over a stationary hot spot (*1*), the Hawaiian-Emperor bend (HEB) has conventionally been interpreted to signify a major change in the motion of the Pacific plate (*2*). The HEB is geographically bounded by the ~47.9 Ma (million years ago) Kimmei Seamount and the ~46.7 Ma Daikakuji Guyot, but as the ~47.9 Ma age of the Kimmei Seamount dates its post-shield stage, inception of the bend could have been as early as 50 Ma (*3*). Broadly contemporaneous early Eocene restructuring of plate kinematics in the Pacific has been recognized in the reorganization of the South Pacific triple junction at magnetic anomaly chron 22-21 (~49.3 to 45.7 Ma), the development of Farallon-Pacific fracture zone bends at chron 24-21 (54.0 to 45.7 Ma), and the redirection of Pacific-Kula spreading at chron 24-20 (54.0 to 43.4 Ma) (*4*). However, as ridges represent comparatively passive features of the plate-mantle dynamic system, geometric modifications to ridge and fracture zone trends are manifestations of a plate reorganization event, and not the causal mechanism.

According to the geometry of the Hawaiian-Emperor chain, the Pacific plate's northwest-directed motion of the last ~47 Ma was preceded by approximately north-directed motion from at least 80 Ma, with a sharp switch at HEB time. Intuitively, one may expect that a switch from north- to northwest-directed motion was instigated by a "pull" from the west, and it has been proposed that subduction spontaneously initiated beneath the Izu-Bonin-Marianas arc and the Tonga-Kermadec arc in the early Eocene (*3*). However, elsewhere along the eastern margin of Asia, there is evidence that subduction was occurring in the Late Cretaceous and Paleocene leading up to the HEB (*5*). Moreover, although spontaneous subduction initiation is expected to commence under a state of tension (*6*), Sutherland *et al.* (*7*) report widespread compression associated with Eocene Tonga-Kermadec subduction initiation, suggesting that it was externally forced. Whittaker *et al.* (*4*) suggested that the reorganization could have been driven by near-parallel subduction of the Izanagi-Pacific ridge beneath eastern Asia in the late Paleocene–early Eocene (Fig. 2), but the evidence reported for ridge subduction is ambiguous. Equally puzzling is the apparent onset of north-dipping subduction of the Pacific plate beneath the Aleutian arc (Fig. 1) at HEB time (*8*), which, intuitively, should have presented a northward pull at approximately the time that the plate motion switched from north-directed to northwest-directed.

Partly due to these problems, but also to unambiguous evidence of hot spot mobility from paleomagnetism (*9*) and plate circuit analyses (*10*), there has been a turn toward explaining the HEB by southward drift of the Hawaiian hot spot, and recently, that has been proposed to play a dominating role (*11*). However, a simple geometric analysis (*12*) showed that the HEB could not have been produced by southward migration of the Hawaiian hot spot alone and that a change in the direction of the Pacific plate's motion around 47 Ma is requisite to explain its formation.

The orientation, length, and age of the Emperor chain coupled with estimates of southward drift of the Hawaiian hot spot (*13*) reveal that, before the HEB, the Pacific plate was drifting northward at an average rate of ~5 cm/year since at least 80 Ma. According to most contemporary plate models (*14*, *15*), during the Late Cretaceous to Paleocene, the Pacific plate was bounded to the north by the Izanagi-Pacific ridge (Fig. 2), the last preserved marine magnetic anomaly from which formed at ~121 Ma (chron M0). Thus, from 80 Ma to HEB time, the northward drift of the Pacific plate implies that it was drifting toward that divergent boundary, which is surprising, both because large, fast-moving oceanic plates are normally assumed to be driven by marginal subduction and because ridges are expected to exert a "push" on a plate (*16*). What could have caused such a large plate to move in the direction of an extensive and fast-spreading ridge? Dominating ridge push from the far (southern) side of the Pacific plate seems unlikely, because that divergent boundary was only about half the length of the Izanagi-Pacific ridge at 80 Ma, and the Pacific-Farallon ridge, although extensive, was oriented north-northwest–south-southeast and so cannot viably explain the Pacific plate's northward course.

RESULTS

The continental rim of the northwest Pacific is decorated by exotic Late Cretaceous–Paleogene island arc rocks—now extending over 3000 km from Hokkaido, Japan, and southern Sakhalin (*17*), across Kamchatka

[1]Centre for Earth Evolution and Dynamics, University of Oslo, Oslo, Norway. [2]Helmholtz Centre Potsdam, GFZ, Potsdam, Germany. [3]Geodynamics Team, Geological Survey of Norway, Trondheim, Norway. [4]School of Geosciences, University of Witwatersrand, Johannesburg, South Africa.
*Corresponding author. Email: mathewd@geo.uio.no

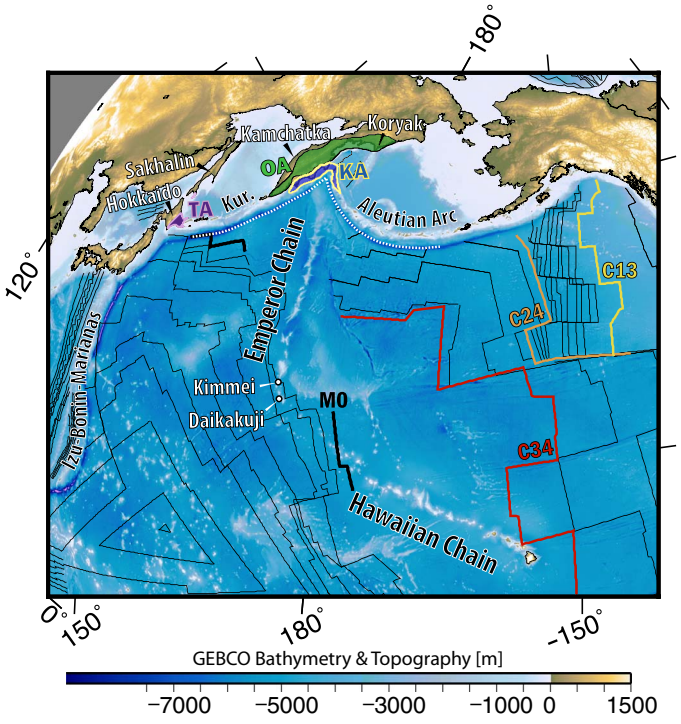

Fig. 1. Bathymetry and topography of the northwest Pacific (GEBCO 2014, www.gebco.net). Thin black lines are isochrons from Seton *et al.* (*14*), and dense isochrons between chrons 24 and 13 (this study) are based on global magnetic anomaly picks (*35*). Isochron M0 south of the Kuril (Kur.) Trench is interpreted from the World Digital Magnetic Anomaly Map (2007) (www.wdmam.org). White dashed line highlights the Kuril and Aleutian trenches as reconstructed in Fig. 3. Labeled place names are mentioned in the text. KA, Kronotsky arc; OA, Olutorsky arc; TA, Tokoro arc.

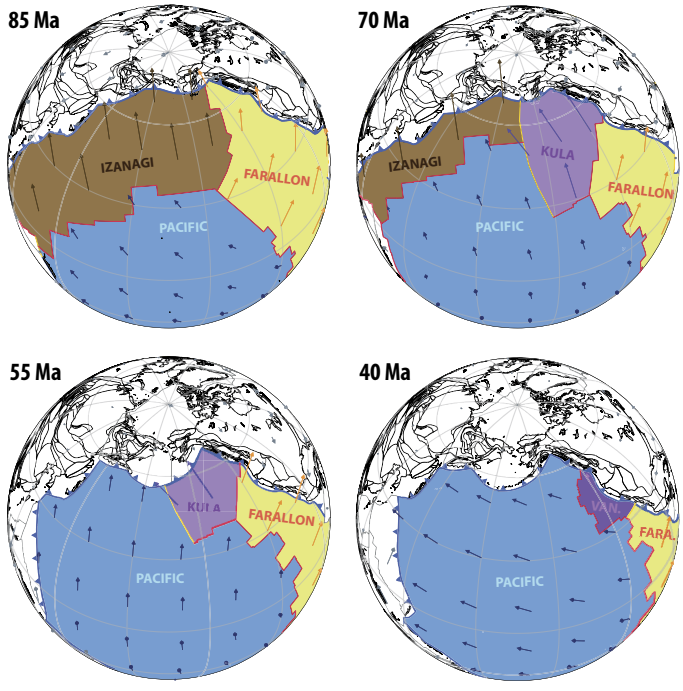

Fig. 2. Conventional Late Cretaceous–Eocene reconstructions of the North Pacific realm. In these reconstructions, the Pacific-Izanagi ridge persists at the northern edge of the Pacific plate until being subducted at ~55 Ma. The Pacific plate shows northerly motion from ~80 to 47 Ma (toward the Pacific-Izanagi ridge) and northwesterly motion after 47 Ma. Mantle reference frame reconstructions, plate boundaries, and velocities according to Müller *et al.* (*15*).

to the Koryak Highlands of Russia (*18*, *19*)—whose accretion history is not explained by conventional tectonic models of the Pacific (*14*, *15*), wherein subduction is restricted to the east continental margin of Asia (Fig. 2). Those rocks comprise at least three intraoceanic arc complexes, namely, TA, OA, and KA (Fig. 1), all of which became active by Campanian time (83.6 to 72.1 Ma) (*17*, *19*, *20*). Late Cretaceous paleomagnetic data from those intraoceanic arcs indicate that they originated at mid-latitudes, ~12° to 22° south of their expected locations, had they been fixed to continental Asia (table S1) (*21*, *22*). Such an extensive intraoceanic subduction system, developed far from a continental margin, could be expected to leave a distinct seismic velocity anomaly in the mantle, and an array of prominent positive *P* and *S* wavespeed anomalies is observed in the upper half of the lower mantle (depths of ~700 to 1400 km) beneath the North Pacific (Fig. 3).

DISCUSSION

Paleomagnetic data from the OA reveal that, by the late Paleocene–early Eocene, the arc had moved above 60°N, arriving to similar latitudes as western Kamchatka at that time (*22*). The rapid northward migration of the active OA in latest Cretaceous to Paleocene time, coupled with the apparent passivity of the northeast margin of Asia following termination of the Okhotsk-Chukotka continental margin arc in the Late Cretaceous (*23*, *24*), suggests that subduction was south-dipping below the OA, allowing northward rollback of the OA trench (Fig. 3). An equally rapid Late Cretaceous–Paleocene northward motion of the TA could imply that those arcs were correlative, forming a continuous north-facing intraoceanic active margin, and their northward drift is moreover compatible with the Late Cretaceous–Paleocene displacement of the Pacific plate. Thus, we propose that, from at least 80 Ma, the northwestern boundary of the Pacific plate comprised a south-dipping intraoceanic subduction zone rather than the Pacific-Izanagi ridge, and we consider the Late Cretaceous–Paleocene northward motion of the Pacific plate to have been instigated and accommodated by retreat of the OA-TA trench. This is compatible with seismic tomography that shows northward-advancing positive wavespeed anomalies beneath the reconstructed OA and TA between depths of 1400 and 900 km (~80 to 50 Ma; Materials and Methods).

By the late Paleocene, trench rollback had brought the OA and TA within a few hundred kilometers of northeast Asia, allowing initial sediment exchange (*25*). Continued convergence resulted in early Eocene arc-continent collision (*24*) and the termination of south-dipping subduction. Subduction ultimately reinitiated on the outboard side of the accreted arc, but with an inverted (north-dipping) polarity, coincident with the initiation of the north-dipping Aleutian subduction system. Subduction polarity inversion following arc-continent collision is anticipated because the backarc lithosphere, having been warmed, thinned, and weakened by previous subduction-related mantle advection, should be easy to rupture (*6*). However, because the backarc lithosphere is warm and thin, the newly established subduction system will not wield the same slab pull force as the system it replaced, altering the plate boundary force balance. As west-dipping subduction beneath eastern Asia (south of the Okhotsk-Chukotka margin) was already ongoing from the Late Cretaceous–Paleocene, the termination of south-dipping intraoceanic subduction would have increased the relative contribution of westward slab pull to the total force balance

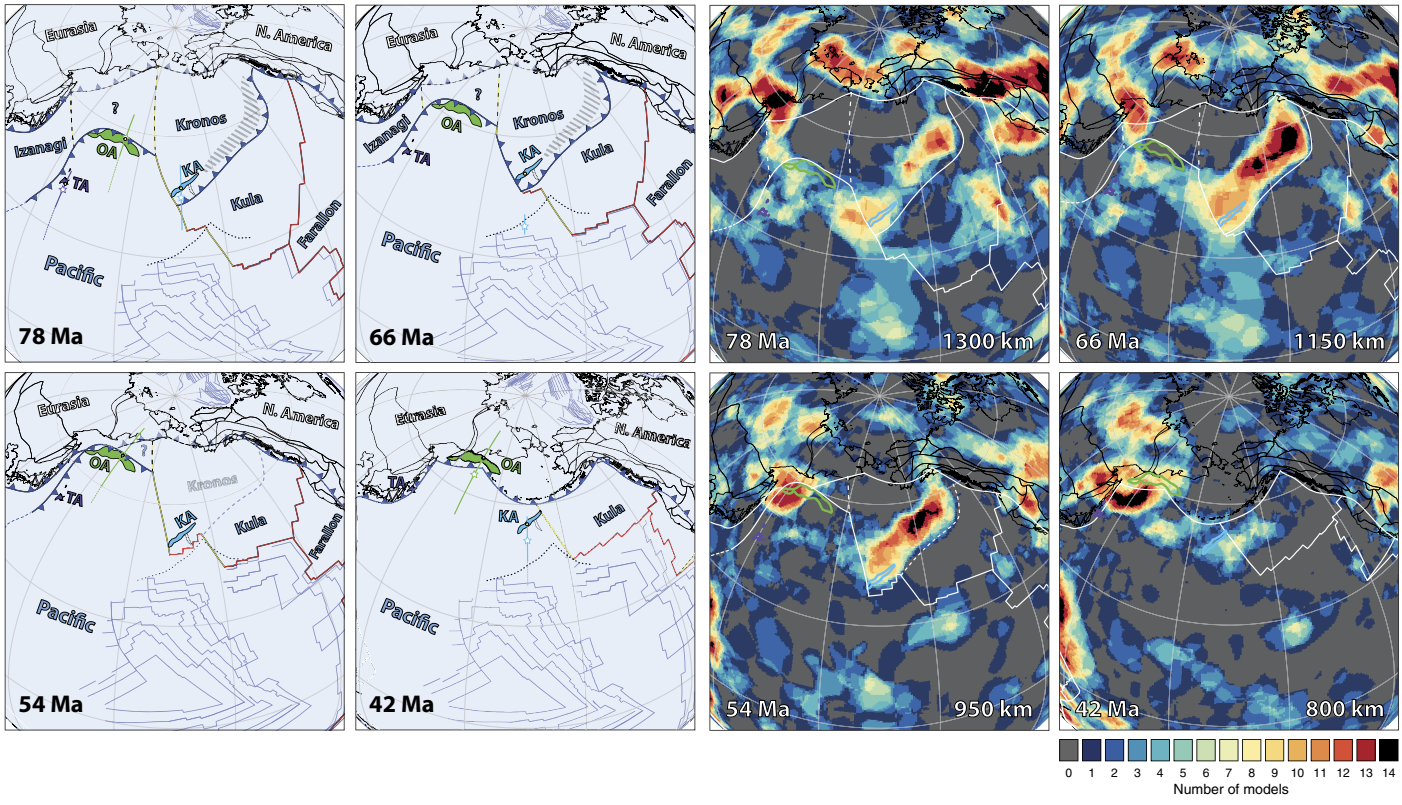

Fig. 3. Alternative Late Cretaceous–Eocene reconstructions. Our model presented in a paleomagnetic reference frame (*32*) (**left**) and a mantle reference frame (*13*) (**right**), using newly defined plate boundaries based on geologic, paleomagnetic, and tomographic data; the remaining boundaries are from Seton *et al.* (*14*) (Materials and Methods). The retrodeformation of terranes was not attempted, except for a simplified unbending of the KA (dashed present-day outline). Left: Colored stars show mean paleomagnetically determined paleolatitudes for the intraoceanic arcs, with error margins denoted by longitudinal bars (dashed lines include error from results uncorrected for inclination shallowing); reference paleomagnetic sites for each arc are shown as yellow circles. Preserved (present-day) isochrons (*14*) are shown as thin blue lines, and the reconstructed edge of preserved oceanic crust along the Kuril-Aleutian trench (at present day) is denoted by a dotted black line. The location of the Izanagi-Kronos boundary is unknown, but two possible locations are shown as dashed transforms. Right: Mantle-based reconstruction of our model compared against seismic tomographic data assuming average upper and lower mantle sinking rates (Materials and Methods). Tomographic data shown as positive wavespeed voting maps, where the vote count conveys the number of tomographic models that report a significantly positive wavespeed anomaly (greater than the depth-dependent mean positive value) at a given location (Materials and Methods).

budget of the Pacific plate, causing a rapid kinematic restructuring—and the HEB.

The KA may not have accreted to the east continental margin of Asia until the Miocene (*18*, *25*), and paleomagnetic data indicate that the arc remained at mid-latitudes during the Paleocene and Eocene (*22*). Because both the Pacific and Kula plates were then moving northward (*14*), this latitudinal stability implies that the KA developed along a south-facing active margin, which must have been independent from the postulated OA-TA subduction system. This interpretation is supported by seismic tomography, which reveals a large positive wavespeed anomaly beneath the Late Cretaceous reconstruction of the KA (Fig. 3). The anomaly remains prominent and approximately stationary between depths of ~1300 and 900 km, corresponding to reconstruction times of ~77 to 50 Ma (Materials and Methods), concurring with the Campanian to Eocene activity of the KA. In our model, the KA resided on the Kronos plate (so-named to distinguish it from the KA) from ~80 to 55 Ma, separated from the Pacific and Izanagi plates by transform boundaries, and from the Kula plate by a northwest-dipping subduction zone. Northwest-dipping subduction beneath the KA ceased during the Eocene, and the extinct KA was then transferred to the Pacific plate, which carried it to Kamchatka where it docked in the mid-to-late Miocene.

Given the contemporaneous initiation and apparent proximity of the OA-TA and KA systems in the Late Cretaceous, it is curious that they commenced with opposing polarities, and we surmise that this may have been due to their origination along different plate boundaries. Specifically, given the timing and latitude of the first appearance of the arcs, and the corresponding orientation of the associated tomographic anomalies, we speculate that the OA-TA initiated by inversion of the Pacific-Izanagi ridge, whereas the KA developed by inversion of the northeast-oriented Izanagi-Farallon ridge (*14*). Subduction initiation by ridge inversion has been recognized elsewhere (*26*, *27*) and can explain the rupture of oceanic lithosphere against the fabric of ocean transforms, which is otherwise unexpected (*6*). Inversion of the Izanagi-Farallon ridge at ~80 Ma may also explain the enigmatic formation of the Kula plate at that time.

With inversion of both the Pacific-Izanagi and Izanagi-Farallon ridges, a string of intraoceanic subduction zones spanned the width of the North Pacific Ocean (Fig. 3). South-dipping subduction along the northern margin of the Pacific plate enabled its swift northward drift by rapid trench retreat, but the resultant arrival of that trench to the northeast margin of Asia caused a large-scale kinematic reorganization, ultimately driving the trajectory of the Pacific plate northwest. The ~3500-km-long

northeast-southwest–oriented, northwest-dipping subduction zone that nucleated along the Izanagi-Farallon ridge may have instigated the formation of the Kula plate and certainly influenced its kinematics. Relics of this large intraoceanic subduction system are only recognized in the KA so far, although our kinematic model predicts that there should also be vestiges of it further east, in Alaska, if it was not entirely subducted beneath the active margin there. Although beyond the scope of the present study, it is worth noting that to the east of the KA, along the Cordilleran margin of North America, north-directed terrane translations were evidently occurring during Late Cretaceous to early Eocene time (*28*, *29*). The initiation of a northward-dipping intraoceanic subduction system (KA) between two northward-migrating domains (the OA-TA as the leading edge of the Pacific to the west, and the displaced Cordilleran terranes to the east) is thus surprising, but a scenario wherein the KA forms above a south-dipping subduction zone would be inconsistent with the existing paleomagnetic and tomographic observations, as well as the timing of the KA's arrival to Kamchatka. However, although the combined observations from tomography, paleomagnetism, geology, and kinematics provide tight constraints on the time-dependent position of the OA-TA and the polarity of its associated subduction zone, the history of the KA, as postulated here, is certainly less well substantiated and remains an important topic for future research.

MATERIALS AND METHODS

Reported isochron ages are with respect to the timescale of Gradstein *et al.* (*30*), except M0, which is reported from the timescale of Gee and Kent (*31*). Our kinematic model (Fig. 3) is based on the absolute reference frames of Torsvik *et al.* (*32*) and Doubrovine *et al.* (*13*) and uses some plate boundaries from Seton *et al.* (*14*). Reconstruction of the OA, TA, and KA intraoceanic arcs was accomplished iteratively through consideration of paleomagnetic (table S1), tomographic, geologic, and kinematic data. Paleomagnetic data from sedimentary clastic rocks were corrected for inclination shallowing assuming a flattening factor (f) of 0.6 (*32*). However, the lower paleolatitudes implied by the uncorrected data are shown by the dashed extensions of the longitudinal bars in Fig. 3. The arcs were reconstructed to positions within the error of the paleomagnetic data except for during the Paleocene, when ~60-Ma paleomagnetic data from KA would place it over oceanic crust that is preserved at present day (66-Ma reconstruction of Fig. 3). To permit direct comparison between the mantle-based reconstruction and seismic tomography, a mean globally averaged sinking rate of 2.0 and 1.5 cm/year was assumed for the upper and lower mantle, respectively, in accordance with global mean average slab sinking rates (table S2) (*33*). Seismic tomographic data from 14 global *P*- and *S*-wave models (table S3) were used to construct positive wavespeed vote maps (*34*) to highlight robust positive wavespeed structures possibly related to subducted lithosphere. Each tomography model was resampled to the same 0.5° latitude-longitude grid and at 50-km-depth increments between depths of 700 and 2850 km. The vote maps were constructed by first removing the layer-dependent mean from each tomography model. The layer-dependent mean positive wavespeed value for each model was then recalculated. A cell in any given model was then assigned a vote of 1 if its associated wavespeed value was in excess of that layer-dependent mean. Finally, the 14 models were stacked so that the vote count of a location conveys the total number of individual model votes at that location (ranging from 0 to 14).

SUPPLEMENTARY MATERIALS

Supplementary material for this article is available at http://advances.sciencemag.org/cgi/content/full/3/11/eaao2303/DC1

table S1. Paleomagnetic data from intraoceanic arcs OA, KA, and TA.

table S2. Example depth-age associations assuming average slab sinking rates of 2.0 and 1.5 cm/year for the upper and lower mantle, respectively.

table S3. Global *P*- and *S*-wave tomography models used to construct the tomographic vote maps shown in Fig. 3.

References (*36*–*53*)

REFERENCES AND NOTES

1. J. T. Wilson, A possible origin of the Hawaiian Islands. *Can. J. Phys.* **41**, 863–870 (1963).
2. W. J. Morgan, Plate motions and deep mantle convection. *Geol. Soc. Am. Mem.* **132**, 7–22 (1972).
3. W. D. Sharp, D. A. Clague, 50-Ma initiation of Hawaiian-Emperor bend records major change in Pacific plate motion. *Science* **313**, 1281–1284 (2006).
4. J. M. Whittaker, R. D. Müller, G. Leitchenkov, H. Stagg, M. Sdrolias, C. Gaina, A. Goncharov, Major Australian-Antarctic plate reorganization at Hawaiian-Emperor bend time. *Science* **318**, 83–86 (2007).
5. H. Sagong, S.-T. Kwon, J.-H. Ree, Mesozoic episodic magmatism in South Korea and its tectonic implication. *Tectonics* **24**, TC5002 (2005).
6. R. J. Stern, Subduction initiation: Spontaneous and induced. *Earth Planet. Sci. Lett.* **226**, 275–292 (2004).
7. R. Sutherland, J. Collot, F. Bache, S. Henrys, D. Barker, G. H. Browne, M. J. F. Lawrence, H. E. G. Morgans, C. J. Hollis, C. Clowes, N. Mortimer, P. Rouillard, M. Gurnis, S. Etienne, W. Stratford, Widespread compression associated with Eocene Tonga-Kermadec subduction initiation. *Geology* **45**, 355–358 (2017).
8. B. R. Jicha, D. W. Scholl, B. S. Singer, G. M. Yogodzinski, S. M. Kay, Revised age of Aleutian Island Arc formation implies high rate of magma production. *Geology* **34**, 661–664 (2006).
9. J. A. Tarduno, R. A. Duncan, D. W. Scholl, R. D. Cottrell, B. Steinberger, T. Thordarson, B. C. Kerr, C. R. Neal, F. A. Frey, M. Torii, C. Carvallo, The Emperor Seamounts: Southward motion of the Hawaiian hotspot plume in Earth's mantle. *Science* **301**, 1064–1069 (2003).
10. I. O. Norton, Plate motions in the North Pacific: The 43 Ma nonevent. *Tectonics* **14**, 1080–1094 (1995).
11. R. Hassan, R. D. Müller, M. Gurnis, S. E. Williams, N. Flament, A rapid burst in hotspot motion through the interaction of tectonics and deep mantle flow. *Nature* **533**, 239–242 (2016).
12. T. H. Torsvik, P. V. Doubrovine, B. Steinberger, C. Gaina, W. Spakman, M. Domeier, Pacific plate motion change caused the Hawaiian-Emperor Bend. *Nat. Commun.* **8**, 15660 (2017).
13. P. V. Doubrovine, B. Steinberger, T. H. Torsvik, Absolute plate motions in a reference frame defined by moving hot spots in the Pacific, Atlantic, and Indian oceans. *J. Geophys. Res. Solid Earth* **117**, B09101 (2012).
14. M. Seton, R. D. Müller, S. Zahirovic, C. Gaina, T. Torsvik, G. Shephard, A. Talsma, M. Gurnis, M. Turner, S. Maus, M. Chandler, Global continental and ocean basin reconstructions since 200 Ma. *Earth-Sci. Rev.* **113**, 212–270 (2012).
15. R. D. Müller, M. Seton, S. Zahirovic, S. E. Williams, K. J. Matthews, N. M. Wright, G. E. Shephard, K. T. Maloney, N. Barnett-Moore, M. Hosseinpour, D. J. Bower, J. Cannon, Ocean basin evolution and global-scale plate reorganization events since Pangea breakup. *Annu. Rev. Earth Planet. Sci.* **44**, 107–138 (2016).
16. D. Forsyth, S. Uyeda, On the relative importance of the driving forces of plate motion. *Geophys. J. Int.* **43**, 163–200 (1975).
17. A. E. Zharov, South Sakhalin tectonics and geodynamics: A model for the Cretaceous-Paleogene accretion of the East Asian continental margin. *Russ. J. Earth Sci.* **7**, ES5002 (2005).
18. D. V. Alexeiev, C. Gaedicke, N. V. Tsukanov, R. Freitag, Collision of the Kronotskiy arc at the NE Eurasia margin and structural evolution of the Kamchatka–Aleutian junction. *Int. J. Earth Sci.* **95**, 977–993 (2006).
19. E. A. Konstantinovskaia, Geodynamics of an Early Eocene arc–continent collision reconstructed from the Kamchatka orogenic belt, NE Russia. *Tectonophysics* **325**, 87–105 (2000).
20. E. L. Geist, T. L. Vallier, D. W. Scholl, Origin, transport, and emplacement of an exotic island-arc terrane exposed in eastern Kamchatka, Russia. *Geol. Soc. Am. Bull.* **106**, 1182–1194 (1994).
21. M. L. Bazhenov, A. E. Zharov, N. M. Levashova, K. Kodama, N. Y. Bragin, P. I. Fedorov, L. G. Bragina, S. M. Lyapunov, Paleomagnetism of a Late Cretaceous island arc complex from South Sakhalin, East Asia: Convergent boundaries far away from the Asian continental margin? *J. Geophys. Res. Solid Earth* **106**, 19193–19205 (2001).
22. N. M. Levashova, M. N. Shapiro, V. N. Beniamovsky, M. L. Bazhenov, Paleomagnetism and geochronology of the Late Cretaceous-Paleogene island arc complex of the

Kronotsky Peninsula, Kamchatka, Russia: Kinematic implications. *Tectonics* **19**, 834–851 (2000).
23. A. Soloviev, J. I. Garver, G. Ledneva, Cretaceous accretionary complex related to Okhotsk-Chukotka subduction, Omgon Range, Western Kamchatka, Russian Far East. *J. Asian Earth Sci.* **27**, 437–453 (2006).
24. A. V. Soloviev, J. I. Garver, M. N. Shapiro, M. T. Brandon, J. K. Hourigan, Eocene arc-continent collision in northern Kamchatka, Russian Far East. *Russ. J. Earth Sci.* **12**, ES1004 (2011).
25. M. N. Shapiro, A. V. Solov'ev, Formation of the Olyutorsky–Kamchatka foldbelt: A kinematic model. *Russ. Geol. Geophys.* **50**, 668–681 (2009).
26. M. Maffione, C. Thieulot, D. J. J. van Hinsbergen, A. Morris, O. Plümper, W. Spakman, Dynamics of intraoceanic subduction initiation: 1. Oceanic detachment fault inversion and the formation of supra-subduction zone ophiolites. *Geochem. Geophys. Geosyst.* **16**, 1753–1770 (2015).
27. T. E. Keenan, J. Encarnación, R. Buchwaldt, D. Fernandez, J. Mattinson, C. Rasoazanamparany, P. B. Luetkemeyer, Rapid conversion of an oceanic spreading center to a subduction zone inferred from high-precision geochronology. *Proc. Natl. Acad. Sci.* **113**, E7359–E7366 (2016).
28. S. T. Johnston, The great Alaskan terrane wreck: Reconciliation of paleomagnetic and geological data in the northern Cordillera. *Earth Planet. Sci. Lett.* **193**, 259–272 (2001).
29. R. J. Enkin, Paleomagnetism and the case for Baja British Columbia. *Paleogeography of the North American Cordillera: Evidence for and Against Large-Scale Displacements*, J. W. Haggart, R. J. Enkin, J. W. H. Monger, Eds. (Geological Association of Canada Special Paper 46 (2006), pp. 233–253.
30. F. M. Gradstein, J. G. Ogg, M. Schmitz, G. Ogg (Eds.), *The Geologic Time Scale 2012* (Elsevier, 2012).
31. J. S. Gee, D. V. Kent, Source of oceanic magnetic anomalies and the geomagnetic polarity time scale, in *Treatise on Geophysics, Vol. 5: Geomagnetism* (Elsevier, 2007) pp. 455–507.
32. T. H. Torsvik, R. Van der Voo, U. Preeden, C. M. Niocaill, B. Steinberger, P. V. Doubrovine, D. J. J. van Hinsbergen, M. Domeier, C. Gaina, E. Tohver, J. G. Meert, P. J. A. McCausland, L. R. M. Cocks, Phanerozoic polar wander, palaeogeography and dynamics. *Earth-Sci. Rev.* **114**, 325–368 (2012).
33. M. Domeier, P. V. Doubrovine, T. H. Torsvik, W. Spakman, A. L. Bull, Global correlation of lower mantle structure and past subduction. *Geophys. Res. Lett.* **43**, 4945–4953 (2016).
34. G. E. Shephard, K. J. Matthews, K. Hosseini, M. Domeier, On the consistency of seismically imaged lower mantle slabs. *Sci. Rep.* **7**, 10976 (2017).
35. M. Seton, J. M. Whittaker, P. Wessel, R. Dietmar Müller, C. DeMets, S. Merkouriev, S. Cande, C. Gaina, G. Eagles, R. Granot, J. Stock, N. Wright, S. E. Williams, Community infrastructure and repository for marine magnetic identifications. *Geochem. Geophys. Geosyst.* **15**, 1629–1641 (2014).
36. N. M. Levashova, M. N. Shapiro, M. L. Bazhenov, Late Cretaceous paleomagnetic data from the Median Range of Kamchatka, Russia: Tectonic implications. *Earth Planet. Sci. Lett.* **163**, 235–246 (1998).
37. N. M. Levashova, M. L. Bazhenov, M. N. Shapiro, Late Cretaceous paleomagnetism of the East Ranges island arc complex, Kamchatka: Implications for terrane movements and kinematics of the northwest Pacific. *J. Geophys. Res. Solid Earth* **102**, 24843–24857 (1997).
38. D. V. Kovalenko, I. R. Kravchenko-Berezhnoy, Paleomagnetism and tectonics of Karaginsky Island, Bering Sea. *Isl. Arc* **8**, 426–439 (1999).
39. D. V. Kovalenko, Paleomagnetism of Paleogene complexes at the Ilpinsky Peninsula (the southern part of the Koryak Highlands). *Izv. Russ. Akad. Nauk* **5**, 72–80 (1993).
40. D. M. Pechersky, N. M. Levashova, M. N. Shapiro, M. L. Bazhenov, Z. V. Sharonova, Palaeomagnetism of Palaeogene volcanic series of the KamchatskyMys Peninsula, East Kamchatka: The motion of an active island arc. *Tectonophysics* **273**, 219–237 (1997).
41. M. L. Bazhenov, V. S. Burtman, Upper Cretaceous paleomagnetic data from Shikotan Island, Kuril Arc: Implications for plate kinematics. *Earth Planet. Sci. Lett.* **122**, 19–28 (1994).
42. Y. Fukao, M. Obayashi, Subducted slabs stagnant above, penetrating through, and trapped below the 660 km discontinuity. *J. Geophys. Res. Solid Earth* **118**, 5920–5938 (2013).
43. M. Obayashi, J. Yoshimitsu, G. Nolet, Y. Fukao, H. Shiobara, H. Sugioka, H. Miyamachi, Y. Gao, Finite frequency whole mantle *P* wave tomography: Improvement of subducted slab images. *Geophys. Res. Lett.* **40**, 5652–5657 (2013).
44. N. A. Simmons, A. M. Forte, L. Boschi, S. P. Grand, GyPSuM: A joint tomographic model of mantle density and seismic wave speeds. *J. Geophys. Res. Solid Earth* **115**, B12310 (2010).
45. C. Houser, G. Masters, P. Shearer, G. Laske, Shear and compressional velocity models of the mantle from cluster analysis of long-period waveforms. *Geophys. J. Int.* **174**, 195–212 (2008).
46. N. A. Simmons, S. C. Myers, G. Johannesson, E. Matzel, LLNL-G3Dv3: Global P wave tomography model for improved regional and teleseismic travel time prediction. *J. Geophys. Res. Solid Earth* **117**, B10302 (2012).
47. S. Burdick, C. Li, V. Martynov, T. Cox, J. Eakins, T. Mulder, L. Astiz, F. L. Vernon, G. L. Pavlis, R. D. van der Hilst, Upper mantle heterogeneity beneath North America from travel time tomography with global and USArray transportable array data. *Seismol. Res. Lett.* **79**, 384–392 (2008).
48. R. Montelli, G. Nolet, F. A. Dahlen, G. Masters, A catalogue of deep mantle plumes: New results from finite-frequency tomography. *Geochem. Geophys. Geosyst.* **7**, Q11007 (2006).
49. M. L. Amaru, "Global travel time tomography with 3-D reference models," thesis, Utrecht University (2007).
50. J. Ritsema, A. Deuss, H. J. Van Heijst, J. H. Woodhouse, S40RTS: A degree-40 shear-velocity model for the mantle from new Rayleigh wave dispersion, teleseismic traveltime and normal-mode splitting function measurements. *Geophys. J. Int.* **184**, 1223–1236 (2011).
51. L. Auer, L. Boschi, T. W. Becker, T. Nissen-Meyer, D. Giardini, *Savani*: A variable resolution whole-mantle model of anisotropic shear velocity variations based on multiple data sets. *J. Geophys. Res. Solid Earth* **119**, 3006–3034 (2014).
52. S. W. French, B. A. Romanowicz, Whole-mantle radially anisotropic shear velocity structure from spectral-element waveform tomography. *Geophys. J. Int.* **199**, 1303–1327 (2014).
53. S. P. Grand, Mantle shear–wave tomography and the fate of subducted slabs. *Philos. Trans. R. Soc. A* **360**, 2475–2491 (2002).

Acknowledgments: We thank D. Gürer for discussions and S. T. Johnston and an anonymous reviewer for comments that improved the manuscript. **Funding:** This work was supported by the Research Council of Norway (RCN) through its Centres of Excellence funding scheme, project 223272 (Centre for Earth Evolution and Dynamics), and through RCN project 250111.
Author contributions: M.D. and T.H.T. conceived the study. G.E.S. provided the tomographic vote maps. M.D. constructed the plate model. J.J. and C.G. checked the magnetic anomaly interpretation in the North Pacific and constructed new Cenozoic isochrons. All authors contributed to discussions and the writing of the manuscript. **Competing interests:** The authors declare that they have no competing interests. **Data and materials availability:** All data needed to evaluate the conclusions in the paper are present in the paper and/or the Supplementary Materials. Additional data related to this paper may be requested from M.D. (mathew.domeier@geo.uio.no).

Submitted 28 June 2017
Accepted 18 October 2017
Published 8 November 2017
10.1126/sciadv.aao2303

Citation: M. Domeier, G. E. Shephard, J. Jakob, C. Gaina, P. V. Doubrovine, T. H. Torsvik, Intraoceanic subduction spanned the Pacific in the Late Cretaceous–Paleocene. *Sci. Adv.* **3**, eaao2303 (2017).